

Experiments on Turbulence and Settling Down of fine Sediments induced by Pumped Storage Operations in a cuboidal Reservoir

M. Müller¹, G. De Cesare¹ and A.J. Schleiss¹

¹Laboratory of Hydraulic Constructions
Ecole Polytechnique Fédérale de Lausanne
EPFL-ENAC-IIC-LCH, Station 18, CH-1015 Lausanne
SWITZERLAND
E-mail: michael.mueller@epfl.ch

Abstract: Long-term sedimentation of pumped storage reservoirs due to the alternation of turbine and pumping modes is an issue regarding sustainability and reliability of such schemes. Systematic experiments on a cuboidal basin are conducted to study how flow fields, turbulence and settling down of fine sediments are affected by discharge, duration of pumped storage sequences, sediment concentration and intake/outlet location. The experimental setup allows simulating inflowing jet into a reservoir, as well as water extraction from the storage volume.

Prior to physical scaled modelling, several scenarios with and without sediments were simulated in a numerical model. The model performance was optimized analysing simulation parameters and several turbulence models. Simulation results were compared to jet theory and observations in preliminary tests on the hydraulic model, which allowed adapting and optimizing both numerical and experimental setup.

Keywords: Jet, turbulence, flow field, hydraulic and numerical modelling

1. INTRODUCTION

Modern power plants are expected to operate in a wide range of output power with improved efficiency, flexibility and safety. Pumped storage hydropower schemes have gained in importance since they allow storing and generating electricity to supply high peak demands by moving water back and forth between reservoirs at different elevations. Sedimentation of these reservoirs leads to storage loss and deposits of particles in front of intake structures and bottom outlets. Thus, it seriously affects sustainable operation and can also lead to severe security problems. In the context of a project consortium called *HydroNet – Modern Methodologies for Design, Manufacturing and Operation of pumped storage power plants*, a research project consists in the description and the control of sedimentation issues in the reservoirs of such hydropower schemes.

The main phenomena governing reservoir sedimentation, as well as measures against reservoir sedimentation in the catchment area, in the reservoir or at the dam are well described (Morris *et al*, 2008, Nicklow, 2000, Morris & Fan, 1997, Schleiss *et al*, 2010). However, the direct link between sedimentation problems and the more recent pumped storage hydropower projects remains poorly treated. Due to pumped storage operation suspended sediments are transferred from one reservoir of the system to the other and with growing pumped storage activity, flow conditions in the reservoir are alternating from one state to another during relatively short laps of time.

In the framework of a Ph.D. research, prototype measurements at the existing pumped storage plant Grimsel II in Switzerland comprise flow field analysis in front of the intake/outlet structure (Müller *et al*, 2010). Further on, a real time turbidity monitoring system is installed at the pressurized shaft of the plant and allows establishing sediment balances in the scheme and detecting eventual influences of pumped storage activity on sediment concentrations. On a hydraulic model, the influence of fast and repeated change of operation between generating and pumping modes on turbulence and sedimentation process by fine sediments is investigated for a simplified reservoir geometry. It is studied how turbulence and settling down of fine sediments is affected by discharge, duration of pumped storage sequences and the intake/outlet location.

The present paper describes the experimental design and the development of the numerical model and gives results of the preliminary numerical and hydraulic test runs.

2. MAIN JET CHARACTERISTICS

The high velocity flow ejected out of the pressurized shaft or conduit into the reservoir of a pumped storage scheme can be compared to a jet phenomenon, which will be reproduced in numerical and hydraulic modelling. As the two fluids have similar characteristics, the jet is so called submerged. The simulation parameters and turbulence characteristics of the numerical model were optimized based on a comparison between simulation results and jet theory. Therefore the most important notions are mentioned and illustrated hereafter.

For a given pipe diameter d_j , the correspondent outlet section A_0 and a certain discharge Q_0 , the efflux velocity U_0 of a fluid with its viscosity ν can be calculated by the equation of volumetric flow rate (Eq. 1). Two other main characteristics of the jet, momentum flux (Eq. 2) and jet Reynolds number (Eq. 3), are directly linked to this initial velocity U_0 :

$$Q_0 = U_0 A_0 \quad (1)$$

$$M_0 = U_0^2 A_0 \quad (2)$$

$$Re_j = U_0^2 d_j / \nu \quad (3)$$

As shown in Figure 1, the structure of a jet can be divided into three zones. The initial length x_i contains the potential core of a length of 4 to 10 times the pipe diameter, where efflux velocities correspond to those uniformly distributed at the outlet section. In the transition zone, a turbulent shear layer, also called mixing layer, entrains water from the direct vicinity of the jet. The fully developed jet zone starts at a distance of approximately $10 d_j$ from the outlet. It is characterized by a transversal velocity profile which follows the shape of a Gaussian distribution.

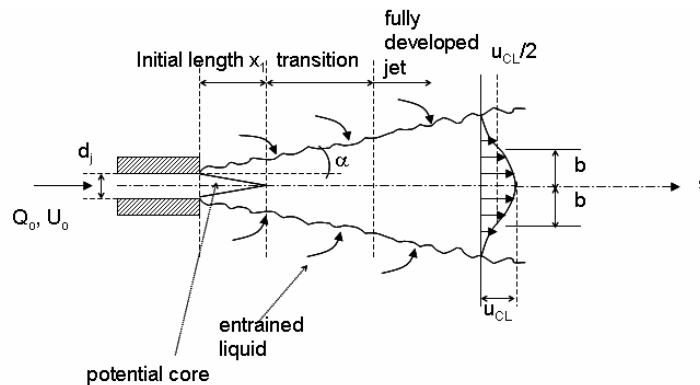


Figure 1 Structure of a submerged jet

In paragraph 4.2, the centreline velocity u_{CL} as well as the transversal velocity $u_t(r)$ of the numerically simulated jet will be compared to the theoretical values given by Jirka (2004), who describes the centreline velocity as a function of the jet momentum flux:

$$u_{CL}(s) = \frac{1}{\sqrt{2\pi}\alpha_{jet}} \frac{\sqrt{M_0}}{s} \quad (4)$$

where α_{jet} is the opening angle of the jet, defined by Jirka as a constant equal to 0.055, and s the distance from the outlet. At the same time Jirka proposes a formula for calculating the transversal velocity profile, using the Gaussian distribution:

$$u_t(r) = u_{CL} e^{-r^2/b^2} \quad (5)$$

$$b = 2\alpha_{jet}s \quad (6)$$

where r is the radial distance from the jet axis and b the transversal distance representing the domain where $u_t \geq 0.37 u_{CL}$.

3. HYDRAULIC MODEL

Systematic experiments in a rectangular horizontal tank shall reveal how repeated changes of IN- and OUT-sequences (corresponding to pumped storage activity in reality) affect turbulence and settling processes in a simplified reservoir configuration. The influence of discharge, cycle duration, initial sediment concentration and intake/outlet position on flow fields, turbulence and settling down of fine sediments is investigated.

3.1. Experimental Setup

The experimental setup (Figure 2a) consists of a cuboidal main basin with a volume of $2.0 \times 4.0 \times 1.5 \text{ m}^3$ and a smaller secondary $1.0 \times 2.0 \times 1.2 \text{ m}^3$ basin. The two reservoirs are connected through a conduit system equipped with a pump and a flow diverter allowing simulating the two exploitation directions defined as follows:

- *IN* (pumping): jet entering the main basin („outlet structure“)
- *OUT* (generating): water flowing out of the main reservoir („intake structure“)

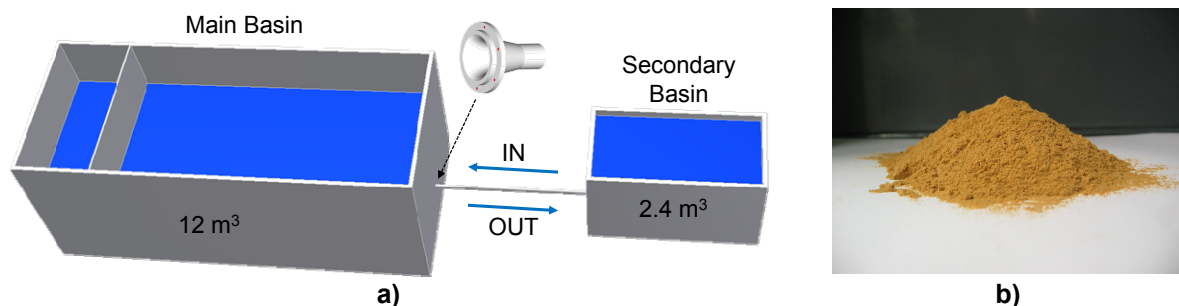


Figure 2 Drawing of the experimental setup with correspondent exploitation directions (a), sediment material employed in the hydraulic model (b)

The intake/outlet is placed on the front wall of the main basin and can be positioned at three different levels. The particular geometry of the trumpet shaped structure limits jet deflection at the outlet and flow irregularities during water extraction.

Semi-rigid plastic pipes connect the secondary basin to the flow diverting system. From there, a rigid PVC pipe of 4.8 cm in diameter and 1.5 m length is connected to the intake/outlet structure of the main basin. Thus, disturbing modelling effects such as pipe irregularities or bends in the approach section can be reduced and the entire pipe system can be easily modified when the intake/outlet level is changed (see 3.2).

Two walls of the main basin are partially made of glass allowing the visualization of the flow conditions in the test volume. The other walls made of steel are painted with a grid of $0.25 \times 0.25 \text{ m}$, providing a reference frame on pictures and films.

Before starting a test run, the two reservoirs are filled by the main circuit of the laboratory and then disconnected from the feeding system. Sediments are added and put in suspension by an air bubble screen placed on the bottom of the two basins, guaranteeing a homogeneous mixture of water and sediments. Then, several IN-OUT-sequences are simulated, during which flow is controlled by a flow meter and a velocity regulator connected to the pump.

A two-dimensional grid of Ultrasonic Velocity Profilers (UVP) allows measuring velocity fields and describing the jet trajectory in the main basin. Thus, the flow conditions and the development of kinetic energy in the reservoir can be monitored and analysed over the entire test period at any moment of the experiment. During the purely hydraulic preliminary tests, the inflowing jet was visualized by colour dye and recorded by two video cameras.

Sediment concentration is measured by two turbidity sensors placed in the main basin and the mixing tank to determine which IN- and OUT-sequences lead to maximum sediment output. In addition, temperature evolution is measured in the two basins.

3.2. Test Parameters

Results of physical modelling aim describing flow fields, turbulence and sedimentation processes in the main basin as a function of four parameters which are varied as follows:

- Discharge Q : five flow rates from 0.3 to 1.1 l/s
- Initial sediment concentration C_0 : 0.3, 0.8 and 1.5 g/l
- Position h of intake/outlet structure : 0.25, 0.50 and 0.75 m above the reservoir bottom
- Specific duration T_P of the IN- and OUT-cycles

The last parameter T_P is defined as the time necessary to fully develop maximum kinetic energy in the main basin and achieve stationary flow conditions ("time to peak"). It depends on flow rate, the operation mode, and possibly also on the two parameters C_0 and h . T_P was determined in numerical simulations for all test configurations to pre-evaluate the time requirements of hydraulic modelling and to reveal differences between the operation modes.

3.3. Sediment characteristics

In the hydraulic model, the fine sediments are reproduced by walnut shell powder (Figure 2b). Experiments performed during former research projects (Kantoush *et al*, 2008, Jenzer *et al*, 2010) revealed satisfying characteristics and behaviour of this homogeneous material for hydraulic modelling concerning reservoir sedimentation. Specific density $\rho_s = 1480 \text{ kg/m}^3$ and a mean particle diameter $d_m = 120 \text{ }\mu\text{m}$ allow reproducing ratios between flow velocities in the basin and settling velocities which can be found in several hydropower schemes.

4. NUMERICAL MODEL

Numerical simulations were carried out for an intake position at $h = 0.5 \text{ m}$ and all flow rates under clear water conditions. Then, an initial sediment concentration of $C_0 = 0.3 \text{ g/l}$ was set in the secondary basin and the case of a sediment laden jet entering into clear water was reproduced for two flow rates. The flow conditions in the main basin were monitored through the evolution of velocity fields generated during IN- and OUT-cycles in three vertical and three horizontal sections of the reservoir.

4.1. Model Characteristics

For numerical modelling, ANSYS software and a CFX solver were employed. The model reproduces the experimental main basin and 0.5 m of the rigid pipe leading water into or out of the reservoir. Depending on the generating or pumping sequence, the pipe extremity is defined as inlet or outlet boundary condition with a fixed mass flow. All vertical faces are considered as walls on which flow velocity is equal to zero. On the free water surface movement is allowed, considering that shear stress and the normal component of velocity are set to zero. Discharge, as well as the inflowing sediment concentration and the initial concentration in the main basin are set by the user, while all other geometrical and hydraulic conditions are either given by the model conception or calculated during the simulations.

Two indicators were studied to determine which calculation time step Δt provides good results within reasonable simulation time. On one hand, the temporal evolution of kinetic energy tells when flow conditions are stable in the test volume and on the other hand, turbulent kinetic energy allows verifying if turbulent phenomena are reproduced adequately.

Simulations showed that kinetic energy converges to a stable value for $\Delta t = 10 \text{ s}$ but this time step leads to severe fluctuations of turbulent kinetic energy. Therefore, $\Delta t = 5 \text{ s}$ has been adopted, giving satisfying results for both kinetic and turbulent kinetic energy evolution.

For simulations with sediments, two drag force models (Schiller-Naumann and Ishii-Zuber) were tested in preliminary simulations and settling velocities of the particles were compared to theoretical values given by the van Rijn equation (van Rijn, 1984). Both models approximate well the theoretical value,

but as the Schiller-Naumann equation (Schiller & Naumann, 1933) considers flow regime during the simulation and sediments are modelled as a dispersed fluid, this model was retained for calculating the drag force coefficient.

4.2. Turbulence Modelling

Previous to numerical simulations of the entire test sequences, several turbulence models available for flow simulation in the CFX module were tested for the case of a jet entering the main basin. Two different families of turbulence models were analysed, eddy viscosity turbulence models on one hand ($k-\epsilon$ and eddy viscosity transport) and Reynolds stress turbulence models on the other hand (explicit algebraic Reynolds stress, EARS). The evaluation of the most adequate turbulence model was based on the analysis of centreline velocity and transversal velocity profiles of the jet, as shown in Figure 3.

Despite from a short core, the $k-\epsilon$ turbulence model fits relatively well to the theoretical values. Soon after the redistribution of flow velocities in the outlet section, the core jet is recognized. In the transition zone, at a distance of 7 to 10 times the pipe diameter, velocity does not decrease as fast as the values given by Jirka. For the eddy viscosity transport model, the calculated core is very short and centreline velocity decreases faster than for the $k-\epsilon$ model leading to lower velocities in the transition zone of the jet. The fully developed jet is well approached for $k-\epsilon$ and eddy viscosity transport models.

The explicit algebraic Reynolds stress model EARS uses algebraic equations to calculate the different Reynolds stress tensor components. Results reveal that the core length and centreline velocities are overestimated in most parts of the jet domain, and that the fully developed jet is well reproduced only for $s/d_j > 20$.

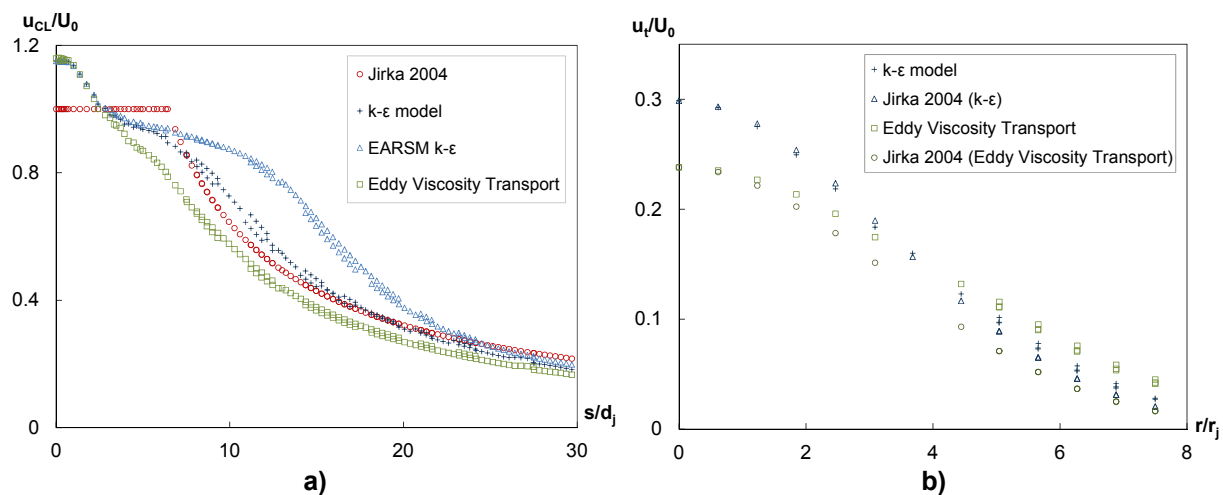


Figure 3 Development of centreline velocity for a jet entering the main basin, $Q = 1.1$ l/s (a), transversal velocity profile at the distance $s = 1.0$ m from the outlet, $Q = 0.3$ l/s (b)

As shown in Figure 3a, the centreline velocity at the outlet is bigger than U_0 . This phenomenon is caused by an asymmetric velocity distribution at the outlet, but does not affect the simulation quality in a significant manner. However, it reveals that the trumpet shaped intake/outlet structure leads to a slightly different evolution of the jet centreline velocity in comparison to a circular nozzle employed in experiments performed by Jirka.

To check the model stability, several flow rates were simulated using eddy viscosity transport, $k-\epsilon$ and EARS turbulence models. The results do not show a significant influence of discharge, neither on the relative core length, nor on the centreline velocity evolution. Consequently, the EARS model was abandoned as it leads to less satisfactory results than the two eddy viscosity turbulence models.

For high flow rates, the comparison of calculated transversal velocity profiles with the expressions given by Jirka reveals that both $k-\epsilon$ and eddy viscosity transport models correctly reproduce the Gaussian distribution. However, for low discharges the eddy viscosity transport model overestimates velocities for $r/r_j > 2$ (Figure 3b) while the $k-\epsilon$ model is more adopted and therefore has been considered to be employed in further numerical simulations.

5. RESULTS AND DISCUSSION

The specific duration T_p to reach stationary flow conditions and constant kinetic energy in the basin was determined for three different sequences (IN, dissipation and OUT) and for each flow rate. Values of $9 \leq T_p \leq 62$ minutes were found depending on discharge and operation mode. T_p is higher for the IN-mode, with the jet evolution requiring more time to develop than the potential flow field towards the intake during the OUT-sequence.

At the beginning of the IN-sequence the jet entering the calm basin generates a fast growth of kinetic energy. After reaching a high energy level, fluctuations appear until values achieve peak energy and stabilize. As mentioned before, the time to establish peak energy differs with discharge, but growth rate up to $E_{kin}/E_{peak} = 0.6$ are similar for every flow rate.

Dissipation requires more time after IN-cycles at high flow rates. For low discharges, the dissipation sequence only lasts a fifth of the time necessary to reach peak energy level. In contrast, almost an entire IN-cycle duration $T_{p,IN}$ is required to regain still water conditions after an IN-sequence at the highest flow rate.

Finally, when water is sucked out of the main basin, kinetic energy develops slower than in the reverse operation mode because velocities start to develop locally in front of the intake and more time is needed to create a stable potential flow field in the entire basin. However, specific duration $T_{p,OUT}$ is less than for the IN-cycle because the relevant phenomena are less turbulent and the evolution of kinetic energy is less affected by fluctuations around the peak value. Thus, for the following simulations the specific duration $T_{p,IN}(Q)$ was adopted for all three cycles, starting with a jet entering the main basin followed by a dissipation cycle and ending with an OUT-sequence.

In the numerical model, the clear water scenarios without sediments reveal similar velocity fields for the IN-sequence and for all tested flow rates. During the development of the jet, two recirculation cells begin to form in a horizontal reservoir section through the jet axis, but flow conditions in the volume are not stationary yet. Once the jet is properly built, the secondary currents in the basin are generally stable in both space and time, with two almost symmetrical recirculation cells in the fully developed jet zone (Figure 4). Towards the end of the IN-sequence, the circulation cells tend to split in two, but no clear separation into four entirely developed cells occurs. The preliminary tests on the physical model where the jet was visualized by colour dye show a stable development of the jet and confirm the results obtained by numerical simulations (Figure 4).

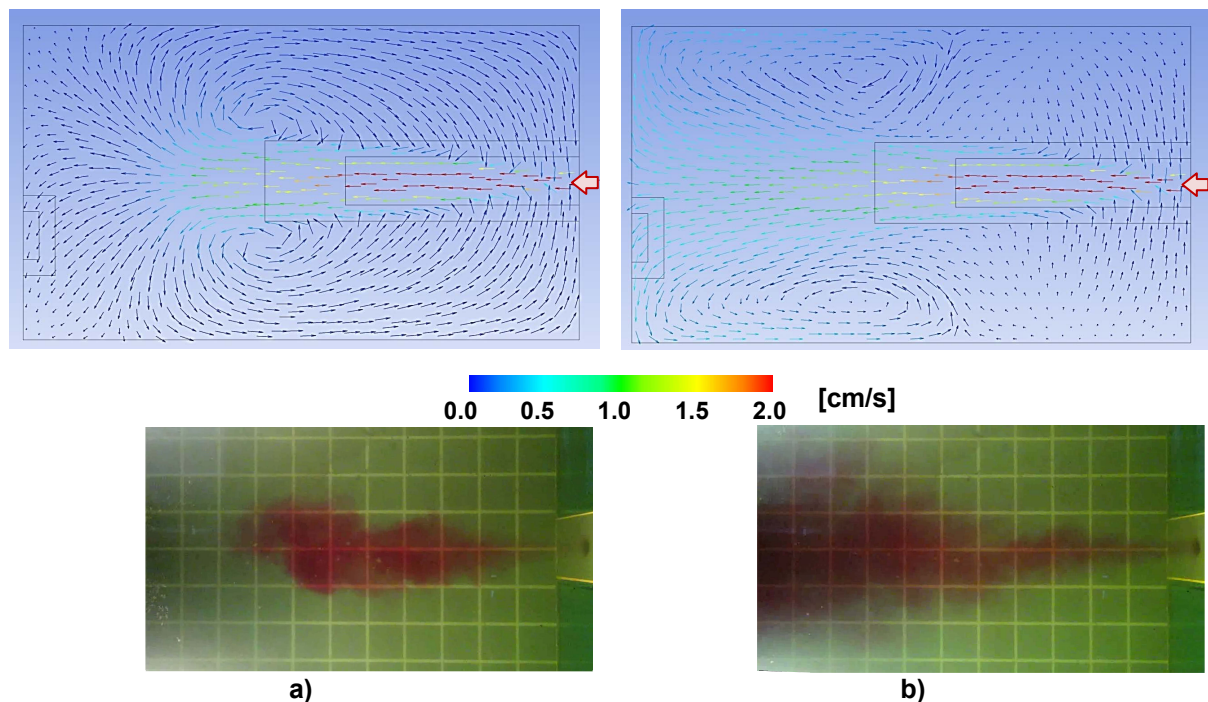


Figure 4 Velocities in a horizontal plane at jet axis level during an IN-cycle (above) and zenith jet pictures for $Q = 0.5$ l/s, at $t = T_p/4$ (a) and $t = T_p$ (b)

In a vertical reservoir section through the jet axis, two circulation cells are observed as well. The upper one is bigger due to the fact that the jet axis is located 0.5 m above the reservoir bottom and the water level in the basin is 1.2 m (Figure 5a). During experiments, both cells are pushed in the jet direction and are located at the far end of the basin towards the end of the sequence.

OUT-sequences generate a potential flow field towards the intake structure which grows faster when high flow rates are drawn out of the test volume. Similar to the IN-cycle, two recirculation cells develop in the back of the basin but very low velocities are observed in this zone.

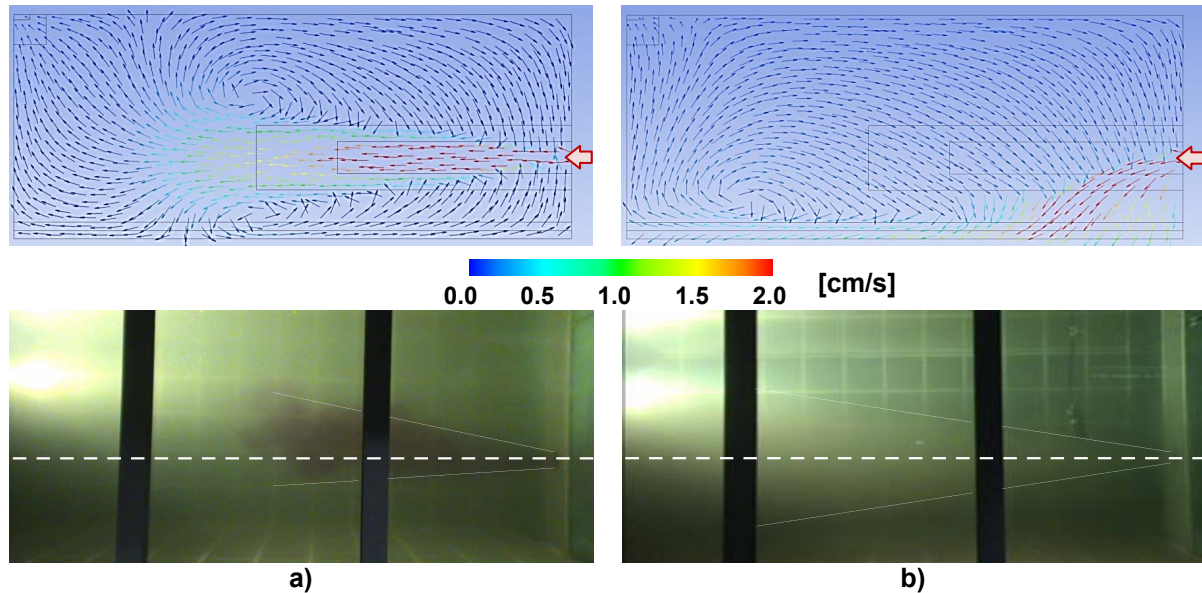


Figure 5 Velocities in a vertical plane at jet axis level during an IN-cycle (above) and lateral jet pictures for $Q = 0.5$ l/s, $C_0 = 0.3$ g/l at $t = T_P/4$, purely hydraulic test (a) and with sediments (b)

Tests with sediments reveal differences between the numerical simulations and the preliminary physical modelling. When the jet entering the basin is composed by a water-sediment-mixture it is slightly deflected towards the reservoir bottom and as soon as the jet is fully developed, recirculation cells start dispersing the particles in the entire test volume. The plunging phenomenon is amplified in the numerical model (Figure 5b), which indicates that settling velocities are overestimated in the simulations. Therefore, the ANSYS model must be adapted in order to be able to improve its functionality for future simulations of test scenarios with sediments.

6. OUTLOOK

As the duration T_P of IN-and OUT-sequences is a key parameter of experiments, the values found by numerical simulations must be confirmed by in the hydraulic model. Thus, UVP velocity measurements will be carried out and the development of the basin overall kinetic energy will show when stationary conditions are reached. Tests on the utility of two UVP sensors with different emitting frequencies were carried out, aiming at determining the most appropriate device for the measurement of flow velocities in the entire basin with a minimum of time shift between each record. During the testing phase of the devices, centreline velocity of the jet was measured for several flow rates. First results confirm the differences observed between the Jirka curve and the values found for the jet entering the cuboidal reservoir. Again, the efflux velocity is higher than the approach velocity in the circular conduit and centreline velocity drops considerably right after the entrance into the basin (Figure 6a).

When T_P is fixed, repeated IN-OUT-Sequences will be simulated in the hydraulic model similar to a square wave as shown in Figure 6b, which allows describing the flow rate Q as a function of time t using Fourier series notation. Starting with the assumption that T_P is equal for the IN- and for the OUT-cycle, the parameter will then be varied to $T_{P,IN}/T_{P,OUT} = 0.5$ and 2.0, respectively, in order to take into account different duration of pumping and generating modes. Similarly, in order to investigate the influence of the time available for developing stable flow conditions in the basin additional tests with

IN-OUT-sequences of 60%, 80% and 120% of T_P will be carried out. Finally, some randomly generated IN-OUT-sequences will be simulated.

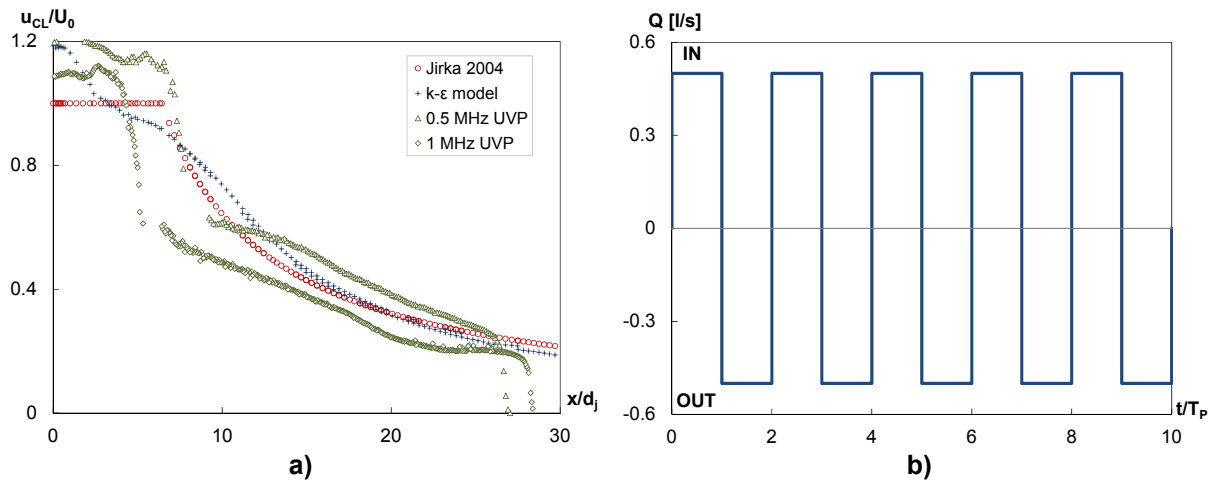


Figure 6 Development of centreline velocity for a jet entering the main basin, $Q = 0.5$ l/s (a), example of IN-OUT-sequence applied in future hydraulic modelling, $Q = 0.5$ l/s, $T_{P,IN} = T_{P,OUT}$

7. ACKNOWLEDGMENTS

The author gratefully thanks the *Swiss Competence Center Energy and Mobility (CCEM)*, *swiss electric research* and *swissenergy – SFOE hydropower research* for funding the project. Mr. Luca Bremen, former Master student at EPFL, contributed to preliminary numerical and hydraulic modelling.

8. REFERENCES

- Jenzer Althaus, J., Schleiss, A.J. and De Cesare, G. (2010), *Measures against Reservoir Sedimentation: Influence of Rotational and Upward Flow on Sediment Behaviour in Reservoirs near Intakes*, Ph.D. Thesis, EPFL, Lausanne.
- Jirka, H.G. (2004), *Integral Model for Turbulent Bouyant Jets in Unbounded Stratified Flows. Part 1: Single Round Jet*, *Environmental Fluid Mechanics*, 4(1), 1-56.
- Kantoush, S.A., Bollaert, E. and Schleiss, A.J. (2008), *Experimental and numerical modelling of sedimentation in a rectangular shallow basin*, *Int. J. of Sed. Res.*, 23(3), 212-23.
- Morris, G.L., Annandale, G. and Hotchkiss, R. (2008), *Reservoir Sedimentation*, in Garcia, M. (Ed) *ASCE Manuals and Reports on Engineering Practice No. 110: Sedimentation Engineering: Processes, Measurements, Modeling and Practice*, ASCE, Reston, Virginia.
- Morris, G.L. and Fan, J. (1997), *Reservoir Sedimentation Handbook: Design and Management of Dams, Reservoir and Watersheds for Sustainable Use*, McGraw-Hill, New York.
- Müller, M., De Cesare, G. and Schleiss, A.J. (2010), *Influence of pumped storage operation on flow conditions near intake/outlet structures: in situ measurements using ADCP*, in Dittrich, Koll, Aeberle & Geisenhainer (Eds) *River Flow 2010*, Braunschweig, September 8-10, 2010, pp. 1139-1145.
- Nicklow, J. (2000), *Optimization of multiple reservoir networks for sedimentation control*, *J. Hyd. Eng.*, 126(4), 232-242.
- Schiller, L. and Naumann, A. (1933), *Über die grundlegenden Berechnungen bei der Schwerkraftaufbereitung*, *Zeitschrift des Vereines Deutscher Ingenieure*, 77, 318–320.
- Schleiss, A., De Cesare, G. and Jenzer Althaus, J. (2010), *Verlandung der Stauseen gefährdet die nachhaltige Nutzung der Wasserkraft*, *Wasser Energie Luft*, Heft 1, 31-40.
- Van Rijn, L.C. (1984), *Sediment Transport, Part II: Suspended load transport*, *J. Hyd. Eng.*, 11, 1613-1641.